



# Influence of surface treatment on defiltration of confined liquid in MCM-41

A. Han, Y. Qiao\*

*Department of Structural Engineering, University of California, San Diego, CA 92093-0085, USA*

Received 21 December 2007; in final form 7 February 2008

Available online 13 February 2008

## Abstract

The effects of post-modification treatment and chlorotrimethylsilane concentration on defiltration behaviors of pressurized liquid confined in a hydrophobic MCM-41 are investigated experimentally. If the chlorotrimethylsilane concentration is relatively low, liquid defiltration can be promoted by extensive drying at elevated temperature or extensive washing at room temperature. If the chlorotrimethylsilane concentration is relatively high, liquid defiltration becomes difficult, while the infiltration volume is larger. These phenomena can be related to the dependence of motion of liquid molecules on structures of nanopore surfaces.

© 2008 Elsevier B.V. All rights reserved.

## 1. Introduction

Although nanoporous materials have been investigated extensively for many decades for catalysis, absorption and adsorption, hydrogen storage, etc. [1,2], developing nanoporous-materials-based mechanical systems, e.g. energy absorption systems (EAS), is still a relatively new area. Energy absorption systems, such as car bumpers, armors, and damping layers, are widely applied in industry for shock absorption, packaging, protection, and earthquake mitigation [3,4]. Nanoporous EAS was initially inspired by the well known phenomenon of dashpot. As a velocity gradient is generated in a viscous liquid, usually by creating relative motion of two solid surfaces, a significant amount of energy can be dissipated due to the internal friction [5]. It was envisioned that, maximizing the solid surface area, e.g. by using a nanoporous material, can be beneficial. Since the specific surface area of a nanoporous material is  $10^2$ – $10^3$  m<sup>2</sup>/g [6], which is larger than that of bulk solids by  $10^5$  times, if the energy absorption efficiency of a dashpot-type device were proportional to its surface area, the viscosity effect can be greatly amplified. However,

experiments on nanoporous silicas, in which water was driven by external loadings to move between compressive parts and tensile parts, demonstrated only marginally improved results [7]. This can be attributed to the later-discovered breakdown of continuum fluid mechanics at the nm scale [8–11]; that is, in a nanopore or nanotube the effective liquid viscosity is much smaller than its bulk counterpart, which can result in rapid liquid transport in a ‘frictionless’ motion. Therefore, the performance of the EAS based on the kinetic effects is lower than the linear projection of results of continuum theory.

Recently, a modified nanoporous EAS has drawn increasing attention [12–16]. The working mechanism is associated with the thermodynamic effects. The nanoporous material was soaked by liquid only when a high pressure was applied, for which the nanopore surface must be hydrophobic. The degree of hydrophobicity could be controlled either by adjusting network composition, such as the silica/alumina ratio in zeolites [17], or modifying nanopore surface structures, e.g. by creating a monolayer of hydrophobic silyl groups [18–21]. Once the liquid was confined in the nanopores, the solid–liquid contact area largely increased. Since the excess solid–liquid interfacial tension was positive, the system free energy increased significantly. When the external pressure was lowered, there were a few

\* Corresponding author.

E-mail address: [yqiao@ucsd.edu](mailto:yqiao@ucsd.edu) (Y. Qiao).

possibilities of liquid behavior. The first was immediate defiltration [22,23]; i.e. the confined liquid came out of the nanopores as soon as the pressure was reduced to below the infiltration pressure. The second was delayed defiltration [24,25]; i.e. the confined liquid did not come out of the nanopores until the pressure was much lower than the infiltration value. The third was non-defiltration [26,27]; i.e. the liquid was 'locked' inside the nanopores even when the external pressure was decreased to zero. In the first case, no mechanical energy was absorbed in a full loading-unloading cycle, because the excess interfacial tension would be eventually released. Such a system may be applied for energy storage or active control [28,29], but not for protection or damping. In the second case, the liquid sorption curve was hysteretic while the system returned to its initial configuration after unloading. The energy absorption efficiency can be assessed as  $E = (P_{in} - P_{de})V$ , where  $P_{in}$  and  $P_{de}$  are the pressures of infiltration and defiltration, respectively, and  $V$  is the specific nanopore volume. Such a system can be used for continuous energy absorption under cyclic loadings, such as in a damping stage or a vehicle buffer. In the third case, since the liquid did not defiltrate, the energy absorption mechanism worked only at the first loading, and from the second loading the nanopores were deactivated. Such a system is suitable to one-time protection applications, such as vehicle bumpers and armors.

The factors that govern the defiltration behavior of confined liquid in nanopores are still inadequately understood. A few theories have been proposed to explain the experimental results, including the discussions on the gas phase effect [30,31], the irreversibility of effective contact angle [32], and the effect of irregular nanopore structure [33]. However, none of them can capture all the observed phenomena. Before a complete theory can be established, more experiments must be carried out to analyze liquid defiltration under a broader spectrum of conditions.

## 2. Experimental

The nanoporous material investigated in the current study was MCM-41, which was hydrothermally synthesized in a  $\text{SiO}_2/\text{CTAB}/\text{Na}_2\text{O}/\text{NH}_3/\text{H}_2\text{O}$  system [34–36]. The sodium silicate solution (Sigma–Aldrich type 338443 water glass) contained 14% NaOH and 27%  $\text{SiO}_2$ . The template was cetyltrimethyl ammonium bromide (CTAB), with the molecular formula of  $\text{CH}_3(\text{CH}_2)_{15}\text{N}(\text{Br})(\text{CH}_3)_3$  and the molecular weight of 364.45 (Sigma–Aldrich, No. 855820). The sodium hydroxide and ammonium hydroxide solution were obtained from Sigma–Aldrich (No. S5881) and EMD Chemicals (No. AX1303p-5), respectively. In order to achieve the desired composition of 4 parts of  $\text{SiO}_2$ , 1 part of CTAB, 1.1 parts of  $\text{Na}_2\text{O}$ , 0.3 parts of  $\text{NH}_3$ , and 200 parts of  $\text{H}_2\text{O}$  (in moles), 3.64 g of CTAB was first mixed with 10.00 g of distilled water in a polypropylene bottle. During stirring, 0.204 g of  $\text{NH}_4\text{OH}$  was dropped into the mixture. In another bottle, 9.41 g of water glass was mixed

with 16.00 g of distilled water through vigorous stirring. The water glass solution was added into the CTAB solution, and the mixture was stirred vigorously at room temperature for 1 h, after which the pH value was adjusted to 10 by using acetic acid (EMD Chemicals, No. AX0073P-5). Then, 4.997 g of 15 wt.% aqueous solution of sodium chloride (Fisher No. S-271-500) was added and the mixture was stirred for 3 min, until it became a single-phase clear solution. The solution was transferred into an autoclave and heated at 95 °C for three days, and cooled to room temperature in air. Finally, silica particles were filtered, washed with distilled water, dried at 100 °C in air, and calcined at 550 °C for 6 h in air to remove the template, forming nanoporous structures. The synthesized MCM-41 was characterized by a TriStar-3000 Gas Absorption Analyzer by the Barret–Joyner–Halenda (BJH) method. The nanopore size was 2.7 nm and the specific surface area was 1100  $\text{m}^2/\text{g}$ . After each liquid sorption test, the sample was washed and activated at 100 °C for 2 h and its porosity property was measured again by  $\text{N}_2$  sorption at 77 K. No statistically meaningful variations could be detected.

Since the silica nanopore surface of unmodified MCM-41 was hydrophilic, a silane surface treatment was performed to increase its degree of hydrophobicity. After vacuum drying at 100 °C for 24 h, about 2 g of MCM-41 particles were refluxed for 36 h with 100 ml of dry toluene solution of chlorotrimethylsilane. The chlorotrimethylsilane concentration was 2% (low-concentration treatment) or 6% (high-concentration treatment). The temperature was maintained at 90 °C by a hot mantle. During this process, chlorotrimethylsilane molecules diffused into the nanopores and deactivated the hydroxyl sites, forming a dense layer of hydrophobic  $\text{C}_1$  surface groups ( $\text{OSi}(\text{CH}_3)_3$ ) [37]. Then, the MCM-41 samples were washed and dried under different conditions: (1) mild washing, i.e. washing with dry toluene only once or (2) extensive washing, i.e. repeated washing and filtering with dry toluene for three times; followed by (1) mild drying, i.e. drying in air at room temperature or (2) extensive drying, i.e. drying in vacuum at 50 °C.

The pressure induced infiltration tests were performed using a stainless steel cylinder, in which 0.2–0.3 g of surface treated MCM-41 was sealed with 3 g of liquid by a steel piston. The liquid was deionized water or saturated aqueous solution of sodium chloride. The piston was intruded into the cylinder by a type 5582 Instron machine at a quasi-static loading rate of 0.5 mm/min. If the loading rate was adjusted in the range of 0.1–1 mm/min, no variation in sorption curve could be detected. When the inner pressure reached 85 MPa, the crosshead of the Instron machine was moved back at the same speed, and the piston might or might not come out of the cylinder, depending on factors that will be discussed shortly. After the first loading-unloading cycle, similar loading loops were repeated for multiple times with the same loading rate. The liquid sorption curves are shown in Figs. 1–4, where the specific volume change is defined as the space occupied by the piston normalized by the mass of MCM-41.

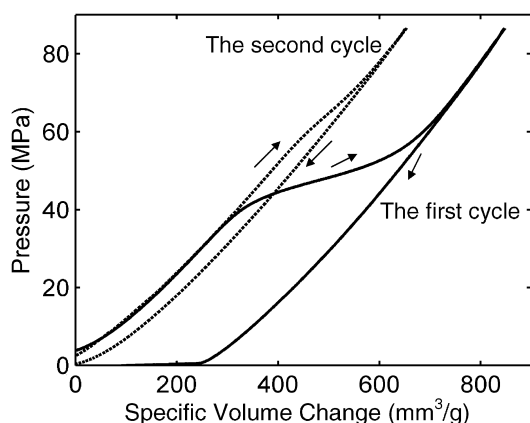


Fig. 1. Infiltration–defiltration curves of saturated sodium chloride solution in MCM-41 treated with low chlorotrimethylsilane concentration. The test is performed after mild washing and mild drying. The curves have been shifted along the horizontal axis.

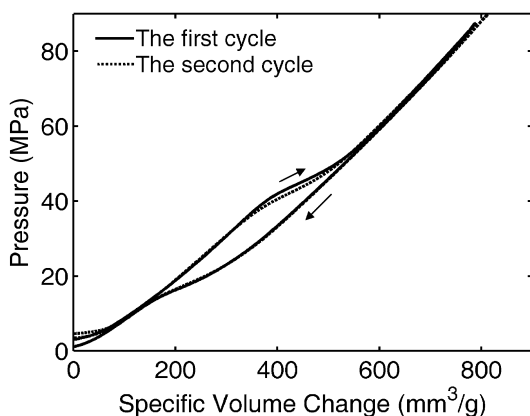


Fig. 2. Liquid sorption curves of saturated sodium chloride solution in MCM-41 treated with low chlorotrimethylsilane concentration. The material has been treated by mild drying after extensive washing.

### 3. Results and discussion

The surface treated MCM-41 particles are hydrophobic. Since they cannot be soaked by liquid spontaneously, they would float on the surface of the liquid. The infiltration and defiltration curves in Fig. 1 are obtained by using saturated sodium chloride solution, and the MCM-41 is modified by low-concentration (2%) chlorotrimethylsilane and then treated by mild washing and mild drying. As a high external pressure,  $P$ , is applied and the capillary effect is overcome, the system volume is compressed. When  $P$  reaches about 40 MPa, the slope of the sorption curve abruptly decreases, indicating that the liquid starts to enter the nanopores. The infiltration ends at about 60 MPa when most of the accessible nanopores are filled. When  $P$  is lower or higher than this range, the system compressibility is much smaller, primarily determined by the bulk modulus of water and the machine stiffness. The sodium chloride is added in the liquid phase as a promoter. In previous experiments [38,39], it was observed that with the addition

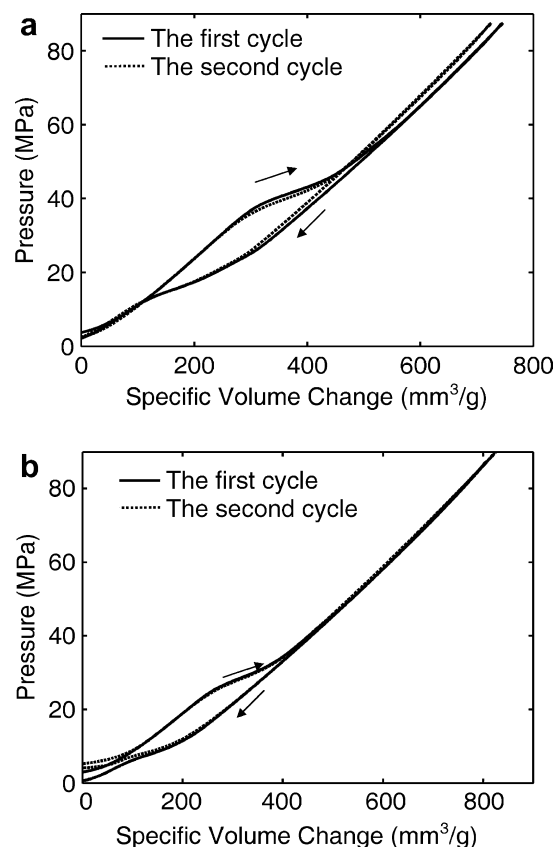


Fig. 3. Liquid sorption curves of (a) saturated sodium chloride solution and (b) distilled water in MCM-41 treated with low chlorotrimethylsilane concentration. The material is treated by extensive drying after mild washing.

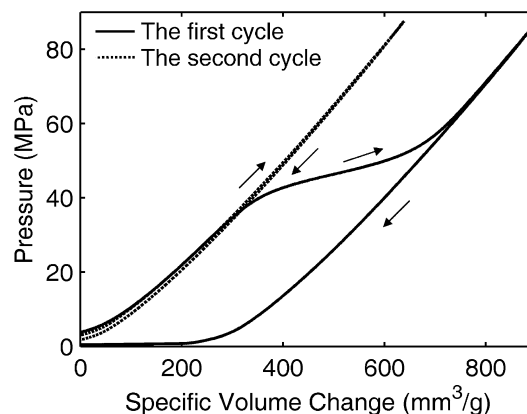


Fig. 4. Sorption curves of saturated sodium chloride solution in MCM-41 treated with high chlorotrimethylsilane concentration. The material has been extensively washed, followed by extensively drying. The curves have been shifted along the horizontal axis.

of electrolyte, probably due to the changes in effective gas solubility and/or molecular structure of solvated ions, it was much easier for confined liquid to defiltrate. However, the testing result on the MCM-41 sample shows that even when the electrolyte solution is saturated, there is still little defiltration. During unloading, the pressure–volume curve is quite linear, which suggests that the confined liquid stays

in the nanopores. This is confirmed by the infiltration–defiltration curves at the second loading. After the first loading cycle completes, when the same pressure is applied again, because the nanopores have already been occupied, little infiltration plateau can be generated. The unclear kink around 60 MPa indicates that the infiltration and defiltration process in a small portion of nanopores is reversible, likely in the smallest nanopores where the infiltration pressure is the highest and the driving force of defiltration is more pronounced than that in larger nanopores. Before and after the infiltration experiment, the gas absorption analyses show that the surface areas of the MCM-41 samples are respectively 765.03 and 734.97 m<sup>2</sup>/g, and the pore volume is respectively 0.76 and 0.75 cm<sup>3</sup>/g; that is, there is only a slight variation (~4%) in porous structure caused by the external pressure and liquid intrusion.

If the MCM-41 is extensively washed, as shown in Fig. 2, even though the processing and surface treatment procedures do not vary, the sorption curves change considerably. During loading, the infiltration still starts at about 40 MPa in saturated sodium chloride solution. However, it ends at about 50 MPa, which should be attributed to that the infiltration volume is reduced by nearly 40%. A more significant change occurs during unloading. When the pressure is reduced to about 25 MPa, defiltration starts, causing the formation of a defiltration plateau parallel to the infiltration plateau. After defiltration completes, the unloading path overlaps with the loading path. After the first infiltration–defiltration cycle, since the confined liquid comes out of the nanopores, the system configuration is similar with the initial condition. Thus, as the pressure is applied again, similar infiltration and defiltration plateaus can be observed, and in all the following cycles the profiles of liquid sorption curves are similar. That is, the motion of the confined liquid is fully reversible in the pressure range under investigation. Clearly, the non-defiltration observed in Fig. 1 is associated with the presence of impurities that cannot be removed by ordinary washing process, such as residual chlorotrimethylsilane molecules and byproduct of hydrochloric acid. After extensive washing and filtering, the nanopore surfaces are dominated by C<sub>1</sub> groups, so that the repelling effect of nanopore wall is pronounced. The reduction in volume of accessible nanopores may be related to the leaching effect; i.e. after extensive washing a portion of surface groups, especially those in relatively large nanopores, are detached from nanopore surfaces.

Fig. 3a shows that the liquid sorption curves of MCM-41 which is extensively dried after mild washing and tested with saturated sodium chloride solution. The infiltration plateau is in the pressure range of 35–45 MPa, and the defiltration plateau is in the pressure range of 20–30 MPa. The infiltration volume is slightly smaller than that of the samples being extensively washed. The second loading–unloading cycle is quite similar with the first one, and in following cycles no significant variation can be detected. While the washing procedure is the same as that of the curves shown in Fig. 1, the vacuum drying effect is

similar with that of extensive washing. Since HCl is highly evaporable and chlorotrimethylsilane is not [40], this result indicates that HCl, which is the byproduct of surface modification reactions, is the dominant impurity that suppresses defiltration. Protons can form strong hydrogen bonds with water molecules. When HCl is attached on nanopore walls, even though the silane groups is hydrophobic, the contaminated areas can be effective hydrophilic. Thus, when water molecules enter nanopores, the system free energy is lowered; that is, the confined water molecules are at a metastable state. As these impurities are removed, either through prolonged washing or accelerated vacuum drying, the nanopore surfaces become clean and the intruded liquid nanocolumns are unstable, leading to the defiltration under reduced pressure.

When the liquid phase is pure water, the main characteristics of liquid sorption curves of vacuum dried MCM-41 remain unchanged (Fig. 3b). An infiltration plateau exists in the loading path and a defiltration plateau exists in the unloading path. The difference between the infiltration pressure and the defiltration pressure is about 15 MPa, similar with that of the sodium chloride based system. The liquid sorption curve does not vary as the loading cycle is repeated. However, the infiltration plateau is in the pressure range of 25–30 MPa, and the defiltration plateau is in the pressure range of 10–15 MPa. The pressure at the onset of infiltration decreases from 35 MPa to about 25 MPa by nearly 30%, which is consistent with the fact that the surface tension of an electrolyte solution is larger than that of pure water [41]. As the cations and ions are removed, the liquid phase becomes effective less polar, and thus the excess interfacial tension between liquid and silane group layer decreases. It can be seen that defiltration is relatively difficult in the pure water based system, since the repelling effect of nanopore surfaces is less profound. If the infiltration and defiltration pressures are further decreased by another 10 MPa, the effective defiltration pressure would become negative. Under this condition, the confined liquid might not be able to defiltrate when  $P = 0$ .

With the chlorotrimethylsilane concentration being increased to 6%, as shown in Fig. 4, no matter whether the sample is extensively washed or extensively dried, or both, no defiltration would occur. The liquid sorption curves are quite similar with that in Fig. 1, except that defiltration is fully prevented and no infiltration can be observed at the second loading. The non-defiltration phenomena may be caused by the relatively non-uniform distribution of C<sub>1</sub> groups. As the chlorotrimethylsilane concentration is increased, the surface modification rate is much higher under the same reaction condition. Hence, along the axial direction of a nanopore, the surface group density tends to be higher close to the open end and lower in the interior, and it may vary from section to section [42]. As a result, local interfacial tension keeps changing when a liquid molecule moves into a nanopore. When the external pressure is lowered, the liquid nanocolumn can be self-

locked due to the ‘ink-bottle effect’, similar with the phenomena observed in mercury porosimetry [43]. It may also be related to the asymmetric variation in effective contact angle during liquid infiltration and defiltration [44].

The dissipated energy caused by the hysteretic infiltration and defiltration process can be calculated as the area enclosed by the load-unloading loop. For the non-defiltration curves in Figs. 1 and 4,  $E$  is nearly 10 J/g. For the defiltration curves in Figs. 2 and 3,  $E$  is about 2 J/g. That is, while the defiltration systems can be used repeatedly as multiple loading cycles are applied, their energy absorption capacity is smaller than that of one-time systems, because of the reduction in  $V$  and the increase in  $P_{de}$ . Note that even the smaller  $E$  value is much larger than that of many conventional damping solids. For instance, the damping efficiency of titanium-nickel alloy is only about 50 mJ/g [45].

#### 4. Conclusions

In summary, through a set of experiments on MCM-41 samples with different surface modification or post-modification treatment procedures, it is observed that the defiltration of confined liquid in nanopores is affected by the chlorotrimethylsilane concentration and the impurities. Only when the nanopore surfaces are covered by uniform surface group layers and of a high purity, defiltration can take place under reduced pressure, for which vacuum drying, extensive washing, and reducing silane agent concentration are of beneficial effects. The systems that work only at the first loading tend to have higher energy absorption efficiency.

#### Acknowledgement

This work is supported by The Army Research Office under Grant No. W911NF-05-1-0288.

#### References

- [1] A. Zukal, Chem. Listy 101 (2007) 208.
- [2] S. Polarz, B. Smarsly, J. Nanosci. Nanotech. 2 (2002) 581.
- [3] S.D. Bartus, J. Adv. Mater 39 (2007) 3.
- [4] D. Jurukovski, M. Petkovski, Z. Rakicevic, Eng. Struct. 17 (1995) 319.
- [5] Z.U.A. Warsi, Fluid Dynamics – Theoretical and Computational Approaches, CRC Press, 1998.
- [6] N.Z. Logar, V. Kaucic, Acta Chim. Slov. 53 (2006) 117.
- [7] Z.S. Chen, F.X. Jiang, J.C.M. Li, J. Mater. Res. 13 (1998) 3275.
- [8] P. Gallo, M. Rovere, E. Spohr, J. Chem. Phys. 113 (2000) 11324.
- [9] G. Hummer, J.C. Rasaiah, J.P. Noworyta, Nature 414 (2001) 188.
- [10] R.M. Lyndenbell, J.C. Rasaiah, J. Chem. Phys. 105 (1996) 9266.
- [11] X.Y. Zhou, H.J. Lu, Chin. Phys. 16 (2007) 335.
- [12] A.Y. Fadeev, V.A. Eroshenko, Study of penetration of water into hydrophobized porous silicas, J. Colloid Interf. Sci. 187 (1997) 275.
- [13] V.D. Borman, A.A. Belogorlov, A.M. Grekhov, V.N. Tronin, V.I. Troyan, Observation of dynamic effects in the percolation transition in a nonwetting–nanoporous body system, JETP Lett. 74 (2001) 258.
- [14] V. Eroshenko, R.C. Regis, M. Soulard, J. Patarin, Energetics – a new field of applications for hydrophobic zeolites, J. Am. Chem. Soc. 123 (2001) 8129.
- [15] X. Kong, F.B. Surani, Y. Qiao, J. Mater. Res. 20 (2005) 1042.
- [16] X. Kong, Y. Qiao, Phil. Mag. Lett. 85 (2005) 331.
- [17] M. Soulard, J. Patarin, V. Eroshenko, R. Regis, Stud. Surf. Sci. Catal. 154 (2004) 1830.
- [18] A. Han, Y. Qiao, Langmuir 23 (2007) 11396.
- [19] A. Han, Y. Qiao, J. Phys. D – Appl. Phys. 40 (2007) 5743.
- [20] A. Han, Y. Qiao, Chem. Lett. 36 (2007) 882.
- [21] S.D. Bhagat, Y.H. Kim, M.J. Moon, Y.S. Ahn, J.G. Yeo, Solid State Sci. 9 (2007) 628.
- [22] N. Desbiens, I. Demachy, A.H. Fuchs, H. Kirsch-Rodeschini, M. Soulard, J. Patarin, Angew. Chem. Int. Ed. 44 (2005) 5310.
- [23] A. Han, Y. Qiao, Appl. Phys. Lett. 91 (2007) 173123.
- [24] X. Kong, Y. Qiao, Appl. Phys. Lett. 86 (2005) 151919.1.
- [25] F.B. Surani, Y. Qiao, J. Appl. Phys. 100 (2006) 034311.1.
- [26] F.B. Surani, A. Han, Y. Qiao, Appl. Phys. Lett. 89 (2006) 093108.1.
- [27] F.B. Surani, X. Kong, Y. Qiao, Appl. Phys. Lett. 87 (2005) 251906.1.
- [28] A. Han, Y. Qiao, J. Mater. Res. 22 (2007) 644.
- [29] Y. Qiao, V.K. Punyamurtula, A. Han, X. Kong, F.B. Surani, Appl. Phys. Lett. 89 (2006) 251905.1.
- [30] Y. Qiao, G. Cao, X. Chen, J. Am. Chem. Soc. 129 (2007) 2355.
- [31] A. Han, X. Kong, Y. Qiao, J. Appl. Phys. 100 (2006) 014308.1.
- [32] T. Martin et al., Dissipative water intrusion in hydrophobic MCM-41 type materials, Chem. Commun. 24 (2002).
- [33] V.D. Borman, A.M. Grekhov, V.I. Troyan, Investigation of the percolation transition in a nonwetting liquid-nanoporous medium system, J. Exp. Theo. Phys. 91 (2000) 170.
- [34] A.C. Voegtlin, A. Matijasic, J. Patarin, C. Sauerland, Y. Grillet, L. Huve, Micropor. Mater. 10 (1997) 137.
- [35] J. Yu, J. Shi, L.Z. Wang, M.L. Ruan, D.S. Yan, Mater. Lett. 48 (2001) 112.
- [36] H. Chen, Y. Wang, Ceram. Int. 28 (2002) 541.
- [37] M.H. Lim, A. Stein, Chem. Mater. 11 (1999) 3285.
- [38] X. Kong, F.B. Surani, Y. Qiao, Phys. Scripta 74 (2006) 531.
- [39] F.B. Surani, Y. Qiao, Phil. Mag. Lett. 86 (2006) 253.
- [40] C.M. Hansen, Hansen Solubility Parameter, CRC Press, 2007.
- [41] S. Hartland, Surface and Interfacial Tension, CRC Press, 2004.
- [42] Y.S. Lin, I. Kumakiri, B.N. Nair, H. Alsyouri, Microporous inorganic membranes, Separ. Purif. Meth. 31 (2002) 229.
- [43] G.T. Shaw, Porosimetry by Mercury Injection, Department of Mines and Technical Survey, Mines Branch, 1963.
- [44] K.L. Mittal, VSP Int. (2006).
- [45] Z.G. Wei, R. Sandstrom, S. Miyazaki, J. Mater. Sci. 33 (1998) 3743.